Optical properties and structural correlations of GeAsSe chalcogenide glasses

Congji Zha · Rongping Wang · Anita Smith · Amrita Prasad · Ruth A. Jarvis · Barry Luther-Davies

Abstract $Ge_xAs_ySe_{100-x-y}$ ($33 \leq x \leq 39$ and $12 \leq y \leq 16$) glasses were prepared, and their structure and optical properties were studied by Raman and UV–Vis-IR spectroscopic techniques. Ge-tetrahedrons [GeSe$_4$] dominated in the structural units, and 'defect' bonds, such as Ge–Ge, Ge–As and As–As bonds, also occurred in the glasses. A structural model for calculation of the optical band gap energy (E_g) of Ge–As–Se glasses was proposed, and the calculated values are consistent with experimental results. Increasing germanium and decreasing selenium content can reduce both the mean bond energies and optical band gap energies, enhancing the photo-sensitivity of the glasses.

1 Introduction

Chalcogenide glasses are promising candidates for photonic applications due to their attractive optical properties, such as high refractive index, high photosensitivity and large optical nonlinearity [1]. Among the different families of chalcogenide glasses, the Ge–As–Se system is of particular interest for two main reasons: the system has a broad glass formation region and the optical nonlinearities of the glasses in this system have been observed to be as high as hundreds of times that of silica glass [2]. The Ge–As–Se system is generally divided into three vitreous domains [3]. In regions I and II,

the number of selenium atoms are sufficient to bond with all the Ge and As atoms, forming [GeSe$_4$] tetrahedral and [AsSe$_3$] pyramidal structural units. The excess selenium atoms exist in the form of Se-Se chains, and the length (l) of the selenium chains for the glasses in regions I and II is $l \geq 2$ and $1 \leq l \leq 2$, respectively. In region III, selenium atoms are insufficient to bond with all Ge and As atoms, thus the formation of ''defect'' or ''wrong'' bonds, such as Ge–Ge and As–As, is necessary so that the unsatisfied Ge and As valences can be satisfied. The glasses formed in region III are more promising, which can be reflected by the fact that some important commercial products, such as AMTIR-1 ($Ge_{33}As_{12}Se_{55}$) and GASIR1 ($Ge_{22}As_{20}Se_{58}$), are all located in this region. It is known that the third order non-linear refractive index (n_2) and optical band gap energy (E_g) of the Ge–As–Se glasses vary significantly with composition [2], and that the glasses containing high germanium content have much higher n_2 values than those with low germanium [3]. Therefore, understanding the correlations of structure and properties of the glasses containing high germanium is of interest. In this paper, chalcogenide glasses, $Ge_xAs_ySe_{100-x-y}$ ($33 \leq x \leq 39$, and $12 \leq y \leq 16$), were prepared from the high germanium vitreous domain (region III) of the Ge–As–Se system, and the influence of composition on glass structure and optical properties was studied by Raman and UV–Vis-IR spectroscopic techniques. The optical band gap energies were calculated, and the correlations of structure and optical properties were discussed.

2 Experimental details

Chalcogenide glasses were prepared in about 50 g batches of arsenic, germanium and selenium metals with purity of 5N (99.999%). Raw materials were weighed within a dry

C. Zha (✉) · R. Wang · A. Smith · A. Prasad ·
R. A. Jarvis · B. Luther-Davies
Centre for Ultrahigh Bandwidth Devices for Optical System,
Laser Physics Centre, Research School of Physical Sciences and
Engineering, Australian National University, Canberra,
ACT 0200, Australia
e-mail: Congji.Zha@anu.edu.au

nitrogen-filled glove box, and the batch was introduced into a pre-cleaned quartz ampoule which was then sealed under vacuum using hydrogen torch. To ensure removal of surface moisture from the quartz ampoule and the batch raw materials, ampoules were baked over-night at 900 °C prior to batching, and the loaded ampoule was dried under vacuum (10^{-6} Torr) at 110 °C for 4 h prior to sealing. The sealed ampoule was placed into a rocking furnace, which was slowly heated to 900 °C at a ramp rate of 300 °C/h. To obtain a good homogeneity of the melt, the ampoule was rocked for 20 h before quenching. The melt was removed from the furnace and air quenched. Rapid cooling is useful for preventing crystallization, and it also helps the glass ingot to strip from the ampoule surface as a result of the large thermal expansion difference of silica and chalcogenide glasses. The quenched ampoule was subsequently returned to a second furnace for annealing for 15 h at a temperature that is slightly below (e.g. 30 °C) the glass transition temperature, T_g, for the purpose of reducing the internal stress of the glass that may be formed during quenching process. The glass transition temperature was measured by using a differential scanning calorimeter (DSC, Shimadzu DSC-50), and no devitrification or crystallization was observed for the samples in this study.

Following the annealing process, the glass was slowly cooled at a rate of 1 °C/min to room temperature. The glass boules were then cut into flat disks of about 2 mm thickness and the facets were ground parallel and polished to optical quality. Raman spectra were measured on a Bruker IFS FT-Raman spectrometer using 1,064 nm excitation from a 1.5 W Nd-YAG laser. The backscattered Raman light was detected by using a liquid nitrogen cooled Ge detector, and the spectral resolution is 1 cm^{-1}. UV–Vis-IR spectra were collected on a Cary 5000 spectrometer using double beams mode.

3 Results and discussion

The Raman spectra of the chalcogenide glasses $Ge_{33}As_{12}Se_{55}$ (HG1), $Ge_{35}As_{15}Se_{50}$ (HG2) and $Ge_{39}As_{16}Se_{45}$ (HG3) are shown in Fig. 1. It can be seen that the Ge–Se vibrations in [GeSe4] tetrahedrons occurred at 193 cm^{-1}, consistent with the results published in [4, 5]. As the content of germanium increases, this band showed a small shift to the low frequency region. The As-Se vibration band generally occurs at around 230 cm^{-1} [4], and this band did not appear in any of the high germanium samples, suggesting that the formation of [AsSe3] pyramids is significantly limited in these glasses. It is known that bond formation occurs in the sequence of decrease in bond energy [6]. The Ge–Se bonds are expected to occur first until all the valences of Ge are satisfied by selenium, because the
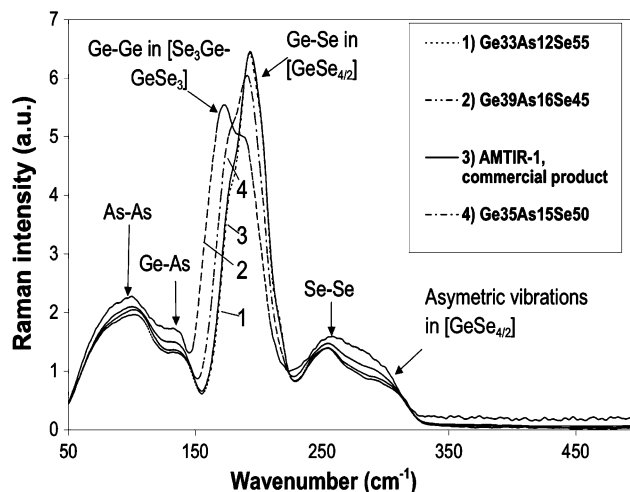

Fig. 1 Raman spectra of high germanium $Ge_xAs_ySe_{100-x-y}$ glasses

Ge–Se bonds have the highest energy in the Ge–Se–As system [6]. Since the number of selenium atoms in these high germanium glasses is insufficient to saturate all the valences of Ge atoms, the possibility of forming As–Se bonds is thus expected to be low. In the higher frequency region, there occurred a weak band at 250 cm^{-1} with a broad shoulder at 300 cm^{-1}, assigned to Se–Se vibrations in Se-chains and asymmetric stretches in [GeSe4], respectively. Considering that Ge–Ge clusters can be formed in the selenium-rich glasses [5], formation of a small amount of Se-Se clusters in these high germanium glasses seems to be understandable. The insufficiency of selenium leads to the existence of unsatisfied Ge and As valences, which must be satisfied by formation of Ge–Ge, As–As and/or Ge–As 'wrong' or 'defect' bonds. The existence of Ge–Ge bonds is indicated by the shoulder occurring in the region 170–180 cm^{-1} at the lower frequency side of the Ge–Se band, assigned to Ge–Ge vibrations in [Se3Ge–GeSe3] structural units [5]. The band at 100 cm^{-1} is assigned to As–As vibrations [4], and its shoulder at 130 cm^{-1} to Ge–As vibrations. By comparing the Raman spectrum of the glass $Ge_{33}As_{12}Se_{55}$ made by our process with the commercial AMTIR-1 (from Amorphous Materials) sample, it can be seen that they are almost identical, indicating that a high accuracy of batching has been achieved with our laboratory fabrication process.

The DSC curves for the chalcogenide glasses are illustrated in Fig. 2, which shows that the glass transition temperature (T_g) increases as the germanium content increases. As germanium has the highest coordination number ($CN = 4$) in the Ge–As–Se system, increasing germanium content is expected to increase the cross-linkage of the glass network. Glass transition temperature usually increases with the connectivity of glass network, and the results in Fig. 2 are consistent with this expecta-
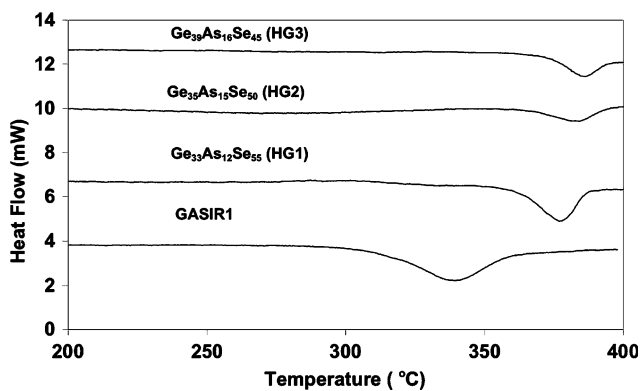
Fig. 2 Influence of composition on DSC curves of high germanium $Ge_xAs_ySe_{100-x-y}$ glasses at a scanning rate of 10 °C/min

tion. All the samples showed a single glass transition peak with no crystallization tendency, suggesting that all the investigated compositions are suitable for glass formation.

It is known that optical band gap energy (E_g) and optical absorption coefficient (α) of glasses can be correlated by equation $\alpha h\nu = A(h\nu - E_g)^{1/2}$, where A is a constant and $h\nu$ is the photon energy [7]. Based on UV–Vis-IR measurement results, the E_g values were calculated and are plotted in Fig. 3. It can be seen that the band gap energy of the Ge–As–Se glasses decreases as the germanium content increases and the selenium decreases. The commercial sample (AMTIR-1) and the glass $Ge_{33}As_{12}Se_{55}$ showed little difference in their E_g curves, further demonstrating that our laboratory fabrication of chalcogenide glasses with the standard sealed quartz ampoule technique can achieve a high accuracy.

Germanium was reported to have some ''contradictory'' effects on the E_g values of various Ge–As–Se glasses. For instance, the E_gs of the high germanium glasses $Ge_xAs_ySe_{100-x-y}$ formed in region III were also observed to

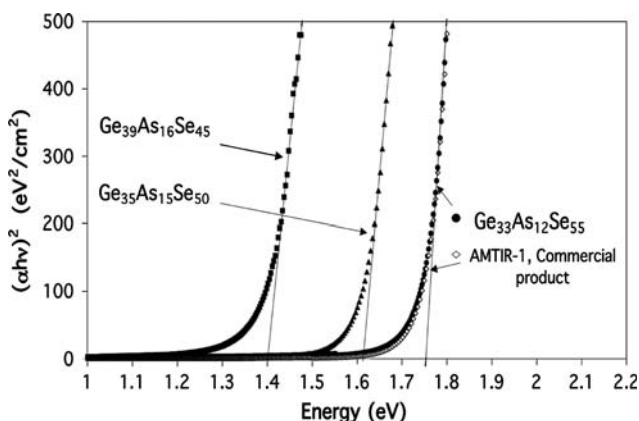decrease as the content of germanium increases in references [2] and [6]. In the $Ge_xAs_{40-x}Se_{60}$ glasses however, E_g was reported to increase with the content of germanium [7]. To understand the correlations of structural and optical properties, a structural model for calculating the bond distribution fractions and optical band gap energies of Ge–As–Se glasses was proposed. As selenium is at a substoichiometric level, we could assume that in the high-germanium and selenium-deficient glasses, Se–Se bonds are negligible and the excess valences of Ge have the same ability to form Ge–Ge and Ge–As bonds. With this structural model, the bond distribution fractions of $Ge_xAs_ySe_{100-x-y}$ glasses can be calculated, and the calculated results are reported in our previous paper [8]. With the bond energies of Ge–Se, Ge–Ge, Ge–As and As–As bonds (known to be 49.4 kcal/mol, 37.6 kcal/mol, 35.6 kcal/mol, and 32.1 kcal/mol respectively [6]), Arsova proposed that the optical band gap energy (E_g) and the mean bond energy ($\overline{E}_s$) can be calculated by

$$E_g = a(\overline{E}_s - b) \tag{1}$$

and

$$\overline{E}_s = \sum_i c_i E_{s(i)} \tag{2}$$

where a and b are constants, c_i is a fraction of the type (i) bond and $E_{s(i)}$ is the bond energy of that bond [7]. The calculated and experimental band gap energies for various Ge–As–Se glasses are described and compared in Fig. 4. The constants, $a = 4.02$ and $b = 1.57$, for empirical Eq. 1 were determined by fitting curve method using the measured E_g values of samples HG1, HG2 and HG3. It can be seen that with this proposed structural model, the calculated E_g values for the high germanium glasses
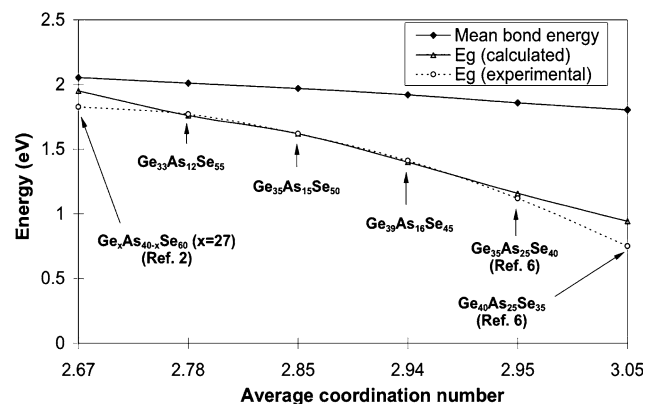

Fig. 3 Plot of $(\alpha h\nu)^2$ versus photon energy ($h\nu$) for of high germanium $Ge_xAs_ySe_{100-x-y}$ glasses

Fig. 4 Comparison of the calculated and experimental band gap energies of high germanium $Ge_xAs_ySe_{100-x-y}$ and $Ge_xAs_{40-x}Se_{60}$ glasses

$Ge_xAs_ySe_{100-x-y}$ are in good agreement with the experimental results. For the selenium-deficient glasses with a formula of $Ge_xAs_{40-x}Se_{60}$, calculation of band gap energy with the equation, $E_g = 2.26 \, (\overline{E_s} - 1.62)$, was proposed by Arsova [6]. This equation was derived based on the assumption that the glass network may be mainly composed of $GeSe_2$ and As_2Se_3. However, in the high-germanium glasses, few As_2Se_3 groups or clusters may be formed. Therefore this equation was found to be not suitable for calculation of the band gap energies of the high germanium glasses described in this study. However, calculating the E_g values of selenium-deficient $Ge_xAs_{40-x}Se_{60}$ glasses with our structural model was found to be appropriate. For instance, the calculated and experimental energy band gap values of the glass $Ge_xAs_{40-x}Se_{60}$ ($x = 27$) are in good consistence shown in Fig. 4. With our structural model, we can calculate the mean bond energy ($\overline{E_s}$) of various Ge–As–Se glasses from the composition, thus the E_g versus composition functions can be derived from Eq. 1. For instance, the E_g versus composition relationship, $E_g = 3.42 - 196.13/(120 + 0.5 \, x)$, for $Ge_xAs_{40-x}Se_{60}$ glasses was successfully derived based on this method. More details about the calculation of the optical band gap energies of various Ge–As–Se glasses will be reported elsewhere.

4 Conclusion

The chalcogenide glasses, $Ge_xAs_ySe_{100-x-y}$ ($33 \le x \le 39$, and $12 \le y \le 16$), in the high germanium vitreous domain of the Ge–As–Se system were synthesized, and their structure and properties were studied. In these glasses, the sub-stoichiometric selenium is insufficient to satisfy all the valences of Ge and As, and bond formation follows a sequence of decreasing bond energy. The structure of these high germanium glasses is dominated by tetrahedral units of germanium. Homo-polar and semi-polar ''defect'' bonds, such as Ge–Ge, Ge–As and As–As bonds, also occurred in the structural units. All glasses showed a single glass transition peak without crystallization tendency. A new equation, $E_g = 4.02 \, (\overline{E_s} - 1.57)$, for calculating the band gap energies of the high germanium glasses was obtained. Increasing the content of Ge and decreasing the quantity of selenium can decrease the optical band gap energy and mean bond energy, thus Ge-rich with selenium-deficient Ge–As–Se glasses are promising for achieving large photosensitivity.

References

1. A.B. Seddon, J. Non-Cryst. Solids **184**, 44 (1995)
2. C. Quémard, F. Smektala, V. Couderc, A. Barthélémy, J. Lucas, J. Phys. Chem. Solids **62**, 1435 (2001)
3. J.T. Gopinath, M Soljačić, E.P. Ippen, V.N. Fuflyigin, W.A. King, M. Shurgalin, J. Appl. Phys. **96**, 6931 (2004)
4. V.S. Vassilev, Z.G. Ivanova, L. Aljihmani, E. Cernoskova, Z. Cernosek, Mater. Letters **59**, 85 (2005)
5. P. Němec, B. Frumarová, M. Frumar, J. Non-Cryst. Solids **270**, 137 (2000)
6. A.A. El-Rahman, A.M. Eid, M. Sanad, R.M. El-Ocker, J. Phys. Chem. Solids **59**, 825 (1998)
7. D. Arsova, J. Phys. Chem. Solids **57**, 1279 (1996)
8. C.J. Zha, B.L. Davies, R.P. Wang, A. Smith, A. Prasad, R.A. Jarvis, S. Madden, A. Rode, Proceedings of ACOFT 2006, pp 31–33, 10–13 July, Melbourne, Australia (2006)